Tensor Magnetothermal Resistance in $YBa_2Cu_3O_{7-x}$ via Andreev Scattering of Quasiparticles

F. Yu,[1] M. B. Salamon,[1] A. J. Leggett,[1] W. C. Lee,[2] and D. M. Ginsberg[1]

[1]*Department of Physics and Science and Technology Center for Superconductivity, University of Illinois at Urbana-Champaign, 1110 West Green Street, Urbana, Illinois 61801-3080*

[2]*Department of Physics, Sookmyung University, Yongsan-gu, Seoul 140-742, Korea*

(Received 31 January 1995)

A magnetic field in the *a*-*b* plane of an untwinned single crystal of $YBa_2Cu_3O_{7-x}$ ($T_c = 92$ K) is found to induce field-dependent off-diagonal elements in the thermal conductivity tensor at 10 K. The principal axes of the field-dependent part of the tensor lie along equivalent ⟨110⟩ directions; a principal component is maximized when the field is along the corresponding principal axis. A model that considers Andreev reflection of thermally excited quasiparticles by vortex screening currents gives semiquantitative agreement with experiment only if the gap function has nodes in the vicinity of ⟨110⟩.

PACS numbers: 74.72.Bk, 74.25.Fy, 74.60.Ec

Although the pairing symmetry of high temperature superconductors remains controversial, there is growing evidence that the gap has nodal structure in the vicinity of $|k_{Fa}| = |k_{Fb}|$, which we will term 45° positions. Photoemission studies on $Bi_2Sr_2CaCu_2O_8$ suggest a single node [1], or perhaps a double node [2], at that point. In $YBa_2Cu_3O_{7-x}$ (YBCO), Josephson tunneling studies [3] are consistent with a π phase change between a and b directions, arguing strongly for a single node. The linear temperature dependence of the penetration depth at low temperatures [4] and the field dependence of the heat capacity [5] also imply line nodes in the gap, while microwave studies [6] indicate that quasiparticles (qp) have much longer mean-free paths in the superconducting state than in the normal state. Taken together, these data suggest that a significant density of qp's exists at low temperatures, and that these are localized near the 45° nodal positions; that is, their crystal momenta are nearly parallel to the ⟨110⟩ axes of the crystal.

In this Letter, we report new thermal conductivity results on untwinned YBCO, exploiting the small phonon thermal conductivity of the cuprates [7] that makes it possible to observe the electronic contribution below T_c. Even at low temperatures ($T/T_c \simeq 0.1$) and in relatively weak fields ($H/H_{c2}^{ab} \simeq 0.003$) applied in the CuO planes, the thermal conductivity is field dependent. More importantly, magnetic fields in the plane induce off-diagonal components of the thermal conductivity tensor $\overleftrightarrow{\kappa}$, the elements of which depend on the magnitude of the field and its angle relative to the crystal axes. With the temperature gradient $(\nabla T)_x$ applied along [100] (the a axis, normal to the chain direction) and the field at an angle ϕ relative to it, a temperature difference ΔT_y is developed along [010], reminiscent of the Hall effect. We ascribe this effect to the scattering of quasiparticles by the screening currents surrounding vortex lines in a manner similar to the scattering of rotons from vortices in superfluid ^{4}He [8].

The sample used in this study is the same untwinned single crystal of YBCO, of dimensions $0.5 \times 0.5 \times 0.02$ mm^3, studied previously [9]. Here, three 12 μm, type E, thermocouple junctions were attached to the sample in the configuration sketched in Fig. 1, to measure the temperature differences ΔT_1 and ΔT_2 along [110] and [1$\bar{1}$0] directions, respectively. The sample was anchored at one end to a Cu heat sink, and a 1 kΩ microchip resistor was attached to the other. With heater power of $\simeq$170 μW, $\Delta T_1 + \Delta T_2$ is less than 0.5 K. The sample was mounted on a closed-cycle refrigerator and placed between the pole faces of a conventional electromagnet. Care was taken to align the c axis of the sample with the rotation axis of the magnet. At each temperature-field-angle setting, 5–20 current-on, current-off sequences were repeated and averaged. Figure 1 shows the *nominal* thermal conductivities determined from ΔT_1 (circles) and ΔT_2 (squares) as functions of ϕ.

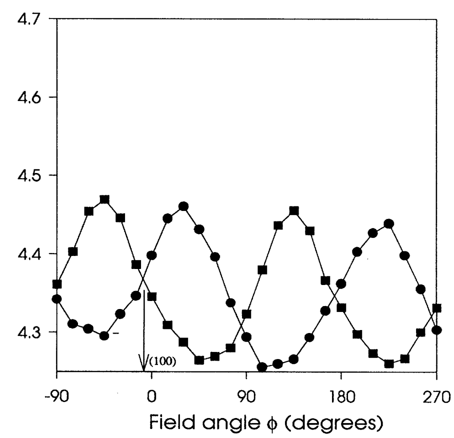

FIG. 1. Nominal thermal conductivities κ_1 (circles) and κ_2 (squares) determined from ΔT_1 and ΔT_2, respectively, vs the field angle ϕ. The lengths used are the vertical separations of the junctions sketched in the inset. The measurements are performed at $T = 10$ K and $\mu_0 H = 1.5$ T.

 0031-9007/95/74(25)/5136(4)$06.00

Nominal means that junction separations $\ell_1 = 0.17$ mm and $\ell_2 = 0.23$ mm along the a axis, as measured from a micrograph, are used. The middle junction is separated by 0.29 mm from the line connecting the outer two, but there is considerable uncertainty in this value due to the finite length of the thermocouple junctions.

While $\triangle T_1$ and $\triangle T_2$ exhibit relatively large changes with field angle, their sum depends only weakly on ϕ. This behavior is consistent with a model in which the field-independent part of $\overleftrightarrow{\kappa}$ has the orthorhombic anisotropy of the crystal [9], while the (small) field-dependent part is also orthorhombic, but with principal axes rotated by 45° (independently of field). To determine the principal components of $\overleftrightarrow{\kappa}$, the anisotropy of which is periodic in ϕ with period π, we must take into account the effective placement of the thermocouples, the sample shape, and the nonuniformity of the heat flow. We do so by computer simulating a square resistor network of 95×81 horizontal and vertical nodes, respectively, approximating the sample shape. Each node is at the junction of a line of $1\ \Omega$ and of $r \times 1\ \Omega$ resistors, running $\pm 45°$ with respect to the vertical axis, as sketched in Fig. 2. Voltage is applied across two horizontal lines of nodes at opposite ends of the array and voltages are measured at three points that match the placement of the thermocouples on the sample. Because of the discreteness of the array, $\triangle V_1$ and $\triangle V_2$ are determined as r is varied over the range $0.8 \leq r \leq 1.2$ for several contact placements. The functional relation $\triangle V_1 / \triangle V_2 = f(r)$ is then determined by interpolation so that $f(1)$ equals the temperature ratio measured in zero field. The principal components κ_{p1} and κ_{p2} of the thermal conductivity tensor are then in the ratio $\kappa_{p1}/\kappa_{p2} = f^{-1}(\triangle T_1/\triangle T_2)$. For each value of r, we determine the ratio g_1/g_{p1}, where g_1 is conductance determined from $\triangle V_1$ and the separation of the contacts in the direction of primary current flow and g_{p1} is the conductance along the principal axis joining the $\triangle V_1$ contacts. This procedure permits us to calculate κ_{p1} from κ_1 in Fig. 1 and κ_{p2} from the ratio.

The field dependence of the principal values is shown in Fig. 2 with the field at 45°, parallel to the principal axis associated with κ_{p1}. That component is essentially independent of field, while κ_{p2} decreases significantly. With the vortex cores situated between conducting planes in this geometry, the arguments used previously [10] to separate phonon and qp contributions by the thermal conductivity can be applied. We fit the field dependence of κ_{p2} by the simple form [11]

$$\kappa_{p2}(H, 10\ \mathrm{K}) = \kappa(\infty) + \kappa_{p2}^{\mathrm{qp}}(0)/(1 + H/H_0), \quad (1)$$

obtaining $H_0 = 12.6$ kOe, $\kappa_{p2}^{\mathrm{qp}}(0) = 0.99$ W/m K, and $\kappa(\infty) = 3.68$ W/m K; the last is attributed to the phonon term. In Fig. 3, we plot the two principal components $\kappa_{p1,2}^{\mathrm{qp}}(1.5\ \mathrm{T}, 10\ \mathrm{K})$ vs the angle φ. The phonon contribution $\kappa(\infty)$ has been subtracted. As was evident from Fig. 1, the thermal conductivity is largest when the magnetic field is parallel to the principal axis in question, and smallest when perpendicular to it. The near equality of the crossing values is circumstantial evidence that nodes involve lines close to 45°.

We have considered, and eliminated, experimental artifacts that might lead to these effects. Nonsuperconducting samples of comparable size and thermal conductivity were studied under the same experimental conditions, and exhibited no field dependence. Misalignment of the plane of rotation of the applied field and the sample plane would produce a c-axis component of the field, giving ΔT_1 and ΔT_2 a twofold angular dependence, but with a constant ratio. Further, vortex lines tend to lock parallel to the CuO planes until the c-axis component of the field in the tilted

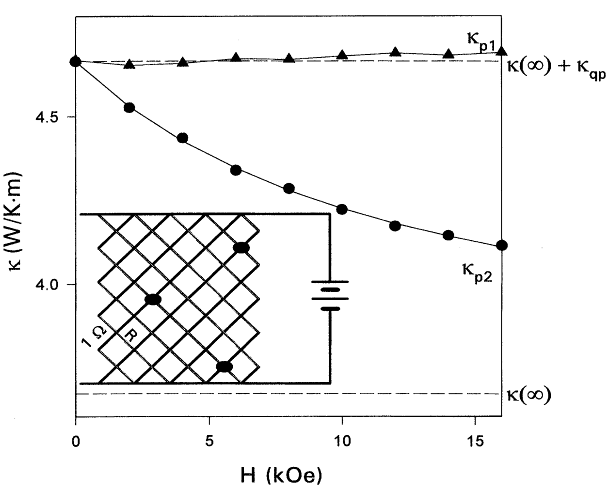

FIG. 2. Field dependence of the principal components of the thermal conductivity with $\phi = 45°$. The solid line is a fit by Eq. (1). The inset is a sketch of the resistor network, showing the voltage contacts.

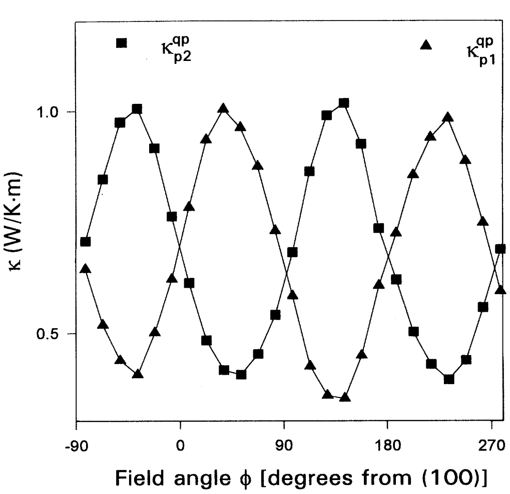

FIG. 3. Full angular dependence of the principal components at 10 K and 1.5 T.

configuration exceeds $H_{c1\perp}$, requiring a misalignment of at least 0.5° before any c-axis component can appear [12].

To determine the effect on κ of Andreev reflection of quasiparticles by the in-plane components of the vortex currents, we assume that the superfluid velocity $\mathbf{v}_s(\mathbf{r})$ associated with these currents varies sufficiently slowly in space that for most of the qp's which carry the heat current an "adiabatic" approximation is legitimate, in which we define the "local" qp energy as viewed from the laboratory frame by

$$E_{\rm lab}(\mathbf{p},\mathbf{r}) = E_{\mathbf{p}-m v_s(\mathbf{r})} + \mathbf{v}_s(\mathbf{r}) \cdot \mathbf{p}\,, \quad (2)$$

where $E_{\mathbf{p}}^2 = (\mathbf{p}^2/2m^* - \mu)^2 + \triangle(\hat{\mathbf{p}})^2$, and we have neglected terms which are of order v_s/v_F relative to those kept. In this approximation the quantity $E(\mathbf{p},\mathbf{r})$ is conserved along the (quasiclassical) qp trajectory, and if as a result at any point the "superfluid-frame qp energy" $E_{\mathbf{p}-mv_s(\mathbf{r})} = [\triangle(\mathbf{p})]$, then at that point Andreev reflection takes place: as viewed from the frame of reference moving with the superfluid, the quasiparticle turns into a quasihole, reversing its velocity and hence its contribution to the thermal current [13]. This mechanism of electronic thermal resistance may be viewed as acting in series with other mechanisms such as impurity scattering. It is clear from Eq. (2) that if a quasiparticle starts from point $\mathbf{r}$, the condition for it to suffer Andreev reflection at point $\mathbf{r}'$ is

$$E_{\mathbf{p}-mv_s(\mathbf{r})} - |\Delta(\hat{\mathbf{p}})| = [\mathbf{v}_s(\mathbf{r}') - \mathbf{v}_s(\mathbf{r})] \cdot \mathbf{p}\,. \quad (3)$$

To obtain an approximate description of the statistics of the quantity $\mathbf{v}_s(\mathbf{r})$, we use a model in which the vortex cores are randomly distributed (after rescaling the axes so as to make the superfluid density isotropic) with mean spacing a_v. Then, for $\rho \equiv |\mathbf{r} - \mathbf{r}'|$ in the range $\xi_0 \ll \rho \ll \lambda_L$ (which for our fields includes the regime $\rho \sim a_v$), a straightforward argument shows that the quantity $\mathbf{v}_s(\mathbf{r}) - \mathbf{v}_s(\mathbf{r}') \equiv \Delta\mathbf{v}_s(\rho)$ is Gaussian distributed with zero mean and variance given by

$$\Delta\mathbf{v}_s^2(\rho) = \frac{\hbar^2}{2m^2 a_v^2}\ln(A\rho/\xi_0)\,, \quad (4)$$

where A is a numerical constant of order unity. Evidently, this behavior is not Markoffian and does not, strictly speaking, allow us to define a "mean-free path" against Andreev reflection.

However, it is clear that we should be able to get at least a qualitative description of the effect by taking $\rho \sim a_v$ in Eq. (4) and hence defining an effective rate of Andreev scattering by vortex currents by

$$\frac{1}{\tau_v(H,\mathbf{p})} = \frac{1}{\tau_{v0}}\exp\left\{\frac{-m^2 a_v^2 [E_{\mathbf{p}} - |\Delta(\hat{\mathbf{p}})|]^2}{p_F^2 \hbar^2 \ln(a_v/\xi_0)\sin^2\psi(\hat{\mathbf{p}})}\right\}, \quad (5)$$

with $\tau_{v0} \sim a_v/v_F$, and where $\psi(\hat{\mathbf{p}})$ is the angle between the direction $\hat{\mathbf{p}}$ and the magnetic field. Here we replace $\mathbf{p} - m\mathbf{v}_s(\mathbf{r})$ in the argument of $E_{\mathbf{p}}$ by $\mathbf{p}$ on the grounds that we will be averaging both over $\mathbf{p}$ and over the superfluid velocity at the "reflecting" point. As it is clear that (the rescaled) a_v^{-2} is proportional to the field H, we evaluate Eq. (5) using

$$p_F^2\hbar^2/m^2 a_v^2 = \pi\gamma\Delta_0^2 H/H_{c2}^{ab}\,, \quad (6)$$

where Δ_0 is the energy gap and γ is a numerical factor which, were we to apply the standard Ginzburg-Landau and BCS relations, would be $(m^*/m)^2$. It should be noted that Eq. (5), being based on the adiabatic approximation, will if anything overestimate the probability of Andreev reflection, particularly for quasiparticles close to the nodes of the gap.

We calculate the qp contribution to the thermal conductivity for heat flow along $\alpha = x, y$ with the thermal gradient along β using a two dimensional version of the usual Bardeen-Rickayzen-Tewordt (BRT) [14] expression,

$$\kappa_{\alpha\beta}^{\rm qp} = \frac{1}{2\pi^2 c k_B T^2 \hbar^2}\int_{p_F}^{\infty} d^2p\,\frac{v_{g\alpha}v_{g\beta}E_{\mathbf{p}}^2}{\Gamma(H,\mathbf{p})}\,{\rm sech}^2\!\left(\frac{E_{\mathbf{p}}}{k_B T}\right), \quad (7)$$

where c is the c-axis lattice parameter and the relaxation rate is given by $\Gamma(H,\mathbf{p}) = 1/\tau_0(\mathbf{p}) + 1/\tau_v(H,\mathbf{p})$. Here, $1/\tau_0(\mathbf{p})$ is the zero-field relaxation rate due to phonon and defect scattering. We consider a single parabolic band with effective mass $m^*/m_e = 2$, and set $E_F = 1$ eV, $k_B T_c/E_F = 0.008$ ($T_c = 92$ K), and $\triangle_0 = (20\ {\rm meV})\tanh(2.2\sqrt{T_c/T - 1})$ [5]; with these parameters, $v_F = 4 \times 10^7$ cm/s. The gap function $\triangle(\mathbf{p}) = \triangle_0 g(\mathbf{p})$ is chosen to be of either d-wave form [15],

$$g_d(\mathbf{p}) = \frac{\cos(p_x a/\hbar) - \cos(p_y a/\hbar)}{1 - \cos(p_F a/\hbar)}\,, \quad (8)$$

or of extended s-wave form for a cylindrical Fermi surface [16],

$$g_{es}(\mathbf{p}) = \frac{1 + \delta([\cos(p_x a/\hbar) + \cos(p_y a/\hbar) - 2J_0(p_F a/\hbar)]/[2J_0(p_F a/\hbar) - 2\cos(p_F a/\sqrt{2}\hbar)])}{1 + \delta}\,, \quad (9)$$

where $J_0(x)$ is a Bessel function. For $\delta > 1$, there are two nodes located symmetrically about the 45° positions.

Making the simplifying assumption that the field-independent relaxation rate $1/\tau_0(p)$ is independent of $\mathbf{p}$ over the narrow energy range of the BRT integral, we calculate $\kappa_{p1,2}^{\rm qp} \equiv \frac{1}{2}(\kappa_{xx}^{\rm qp} + \kappa_{yy}^{\rm qp} \pm 2\kappa_{xy}^{\rm qp})$ from Eq. (7); at $H = 0$ we obtain $\kappa_{p2}^{\rm qp}(0)/\tau_0 = (8.1 \times 10^{11}$ W/m K s) for a d-wave gap. The qp contribution from Eq. (1) gives $\tau_0 = 1.2$ ps compared with $\tau_0 = 5$ ps, estimated from microwave conductivity data on twinned samples [17], which therefore include a contribution from the chains. The extended s-wave gap requires $\tau_0 = 0.26$ ps.

Figure 4 shows $\kappa_{p1}^{\rm qp}(1.5\ {\rm T},\ 10\ {\rm K})$ for both d and extended s gaps, with $\mu_0 H_{c2}^{ab} = 500$ T, $\lambda/\xi = 100$ [18],

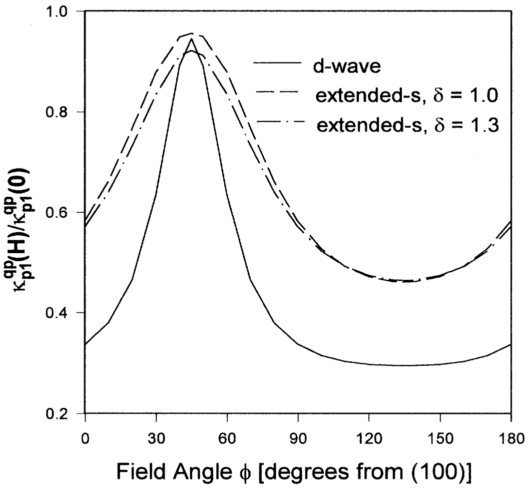

FIG. 4. Calculated ratio of the principal component $\kappa_{p1}(H)$ of the quasiparticle thermal conductivity to its value at zero field for d-wave and extended s-wave gap functions. The parameters are given in the text. For $\delta = 1$, the s-wave node occurs exactly at 45°; for $\delta = 1.3$, two nodes appear at 35° and 55°, respectively.

and $\tau_{v0} = \tau_0/3$ chosen to produce the observed $\simeq 60\%$ modulation in κ_{p1}^{qp}. With $\delta = 1.3$ the extended s nodes are separated by 20°, such as was recently reported for $Ba_2Sr_2CaCu_2O_x$ [2]. In the d-wave case, the characteristic length $v_F\tau_{v0} = 1600$ Å exceeds the vortex spacing $a_v \simeq 400$ Å. That Andreev reflection takes place only if the sign of $\Delta \mathbf{v}_s \cdot \mathbf{p}$ is positive leads to a factor of 1/2 in the relaxation rate; on the other hand, the fact that it reverses, rather than merely annihilates, the heat current leads to a compensating factor of 2. These and other "geometric" factors are all buried in the prefactor τ_{v0}. Clearly, it is not possible to distinguish unambiguously between s- and d-wave gaps from our data. The extended s-wave gaps produce a more symmetric angular variation, as is observed. However, the length $v_F\tau_{v0}$ required to produce the amplitude of the oscillations is $\simeq 160$ Å, less than a_v, making this a less likely possibility.

In summary, we have observed a new Hall-like effect in which Andreev scattering by the screening currents in a type-II superconductor with strong gap anisotropy induces heat flow normal to the temperature gradient. This is to be contrasted with the classical Righi-Leduc effect in which the field is normal to the plane of the heat flow. We have demonstrated that band structure and gap parameters appropriate for YBCO give reasonable estimates of the quasiparticle contribution to the thermal conductivity at low temperatures. With only τ_0 and τ_{v0}/τ_0 as parameters and either a d-wave or an extended s-wave gap function, the model provides an explanation for the induced anisotropy of the thermal conductivity tensor. The model for the relaxation rate is somewhat extreme, resulting in peaking of the thermal conductivity for fields along the nodal lines that is narrower than observed.

This work was supported by the National Science Foundation (Grant No. DMR-91-20000) through the Science and Technology Center for Superconductivity. We are grateful to N. Goldenfeld for useful discussions and assistance with numerical integration.

[1] Z.-X. Shen *et al.*, Phys. Rev. Lett. **70**, 1553 (1993); R.J. Kelley *et al.*, Phys. Rev. B **50**, 590 (1994).
[2] H. Ding *et al.* (to be published).
[3] D.A. Wollman *et al.*, Phys. Rev. Lett. **71**, 2134 (1993); (to be published).
[4] W.N. Hardy *et al.*, Phys. Rev. Lett. **70**, 3999 (1993).
[5] K.A. Moler *et al.*, Phys. Rev. Lett. **73**, 2744 (1994).
[6] K. Zhang *et al.*, Phys. Rev. Lett. **73**, 2484 (1994); D.A. Bonn, P. Dosanjh, R. Liang, and W.N. Hardy, *ibid.* **68**, 2390 (1992); D.A. Bonn *et al.*, Phys. Rev. B **47**, 11 314 (1993).
[7] P.B. Allen, X. Du, L. Mihaly, and L. Forro, Phys. Rev. B **49**, 9073 (1994).
[8] R.A. Ferrell, Phys. Rev. Lett. **68**, 2524 (1992).
[9] R.C. Yu, M.B. Salamon, J.P. Lu, and W.C. Lee, Phys. Rev. Lett. **69**, 1431 (1992).
[10] F. Yu, M.B. Salamon, V.N. Kopylov, N.N. Kolesnikov, H.M. Duan, and A.M. Herman, Physica (Amsterdam) **235–240C**, 1489 (1995); F. Yu *et al.* (to be published).
[11] W.F. Vinen, E.M. Forgan, C.E. Gough, and M.J. Hood, Physica (Utrecht) **55**, 94 (1971).
[12] D. Feinberg and A.M. Ettouhami, Int. J. Mod. Phys. **7**, 2085 (1993).
[13] A.F. Andreev, Zh. Eksp. Teor. Fiz. **46**, 1823 (1964); [Sov. Phys. JETP **19**, 1228 (1964)].
[14] J. Bardeen, G. Rickayzen, and L. Tewordt, Phys. Rev. **113**, 982 (1959).
[15] J.A. Martindale *et al.*, Phys. Rev. Lett. **68**, 702 (1992); N. Balut and D.J. Scalapino, *ibid.* **68**, 706 (1992).
[16] T. Hotta, J. Phys. Soc. Jpn. **62**, 274 (1993).
[17] D.A. Bonn *et al.*, J. Phys. Chem. Solids **54**, 1297 (1993).
[18] S.L. Cooper and K.E. Gray, in *Physical Properties of High Temperature Superconductors IV,* edited by D.M. Ginsberg (World Scientific, Singapore, 1994), p. 122.